Rapid determination of compressive yield stress of dense suspensions by a mean-phi ($\bar{\phi}$) model of high pressure filtration

Sasanka Raha [a], Kartic C. Khilar [b], Pradip [a,*], Prakash C. Kapur [a]

[a] *Tata Research Development and Design Centre, 54B Hadapsar Industrial Estate, Pune-411013, India*
[b] *Dept. of Chemical Engineering, Indian Institute of Technology, Powai, Mumbai, India*

Abstract

The compressive yield stress plays a crucial role in consolidation of concentrated suspensions in sedimentation and thickening, filtration under pressure or vacuum, shaping of ceramic bodies by slip casting, and in disposal of mining and industrial particulate wastes. Measurement of compressive yield stress is ordinarily a time consuming undertaking. Fast and demonstrably reliable techniques for measuring compressive yield stress are needed for screening dispersant/flocculent reagents and establishing their optimum dosage for improving the dewatering characteristics. Fast characterization of yield rheology is also essential in case of biologically active sludges whose rheological behavior changes with time and in monitoring of slurry characteristics for on-line control of industrial dewatering processes in face of fluctuating feeds. We propose rapid methods for determining compressive yield stress from truncated single pressure or truncated step pressure test data by a recently proposed mean-phi ($\bar{\phi}$) model of high pressure filtration. Because filtration rate slows down drastically as the end point is approached, considerable saving in measurement time is possible in truncated tests where the experiment is terminated in single pressure tests or pressure is stepped up to next higher level in multi pressure tests before the filtration system reaches equilibrium or steady state. Based on a recently proposed $\bar{\phi}$-model, we derive and validate a mathematical model for simulation of conventional and truncated step pressure filtration tests. In the former case, the process is permitted to run to equilibrium before the pressure is stepped up. The simulation model is employed to extract compressive yield stress as a function of solid volume fraction from truncated single pressure and step pressure test data. The proposed fast technique is used to demonstrate the effect of pH, polymers and surfactants on compressive yield stress of flocculated and dispersed suspensions.

Keywords: Fast measurement of compressive yield stress; Truncated high pressure filtration; Truncated step pressure filtration; Mathematical models

1. Introduction

There is considerable interest in mathematical modeling of solid–liquid separation processes [1–12]. Many of these models comprise two principal components, namely, material-independent solid–liquid continuity–momentum balance equations and material-specific constitutive equations that relate the characteristic properties of the suspension. The hindered settling function and compressive yield stress (compressibility) have been identified as the material specific key rheological properties in solid–liquid separation. While the former drives the kinetics of dewatering, the latter determines the consolidation behavior of concentrated suspensions in sedimentation or thickening by gravity and centrifugation, filtration under pressure or vacuum, slip casting in ceramic fabrication processes, and in disposal of mining and industrial particulate wastes. The compressive yield stress is a measure of the ability of particle network of a given microstructure to accommodate elastic strain under compressive stress due to the presence of surface forces between suspended particles [2,13–17]. It is especially relevant in high pressure filtration of fine and colloidal suspensions which give rise to compressible filter cakes. For example, Buscall and White [2] and Landman et al. [4–6,8]

developed a sophisticated theoretical framework for pressure filtration in terms of hindered settling and compression rheology. Their governing diffusion equation in one-dimensional filtration under constant pressure ΔP is

$$\frac{\partial \phi}{\partial t} = \frac{\partial}{\partial z}\left[D(\phi)\frac{\partial \phi}{\partial z} - \phi\frac{\mathrm{d}h}{\mathrm{d}t}\right] \quad (1)$$

where $\phi = \phi(z,t)$ is local volume fraction solids at height z, $0 < z(t) < h_t(t)$, above the membrane at filtration time t and $h_t(t)$ is total distance between the membrane and piston. The filtration diffusivity $D(\phi)$, which determines the time scale of the process, is a composite function of a hindered settling factor $R(\phi)$ and compressive yield stress $P_y(\phi)$ of filter cake

$$D(\phi) = \frac{(1-\phi)^2}{R(\phi)}\frac{\mathrm{d}P_y(\phi)}{\mathrm{d}\phi} \quad (2)$$

It is, however, more convenient to calculate the diffusivity by following approximate relationship [6]

$$D(\phi) = \frac{1}{2}\frac{\mathrm{d}\beta^2}{\mathrm{d}\phi}\left(\frac{1}{\phi_0} - \frac{1}{\phi}\right)^{-1} \quad (3)$$

where β is slope of the initial time similarity solution of the filtration equation and ϕ_0 is solid volume fraction in feed suspension. Moreover, the constitutive equation relating stress and deformation of the particulate bed is given by [2]

$$\frac{D\phi}{Dt} = \kappa(\phi)\left(P_p(\phi) - P_y(\phi)\right) \quad (4)$$

where $D\phi/Dt$ is material derivative of local volume fraction solids, $\kappa(\phi)$ is dynamic compressibility and $P_p(\phi)$ $(0 < P_p \leq \Delta P)$ is compressive stress acting on the particle network, which increases with increasing ϕ. After a long time (in theory as $t -> \infty$), consolidation of filter cake ceases and filtration ends as the process reaches equilibrium at uniform volume fraction solid ϕ_∞ when the applied load ΔP is wholly transferred onto the network and equals compressive yield stress; that is,

$$\Delta P = P_y(\phi);\ \phi \rightarrow \phi_\infty. \quad (5)$$

Thus, compressive yield stress determines the theoretical upper limit for removal of water under a given applied pressure. Eq. (5) permits direct measurement of compressive yield stress from pressure filtration test.

Because of the complexity of the phenomenon, it is at present not possible to calculate compressive yield stress from first principles. Buscall and White [2] developed a multiple-speed equilibrium sediment height technique (also known as centrifugal sedimentation) for measuring compressive yield stress. Other methods are pressure filtration, drying consolidation and osmotic pressure [15–19]. The last two techniques are 'pressureless' in the sense that no external driving force is employed. The consolidation behavior in these also differs somewhat from centrifugal sedimentation and pressure filtration methods where a mechanical driving force is imposed for compression [18,19]. It is reasonable to infer that the estimate of compressive yield stress by mechanical consolidation techniques should be more relevant and directly applicable for analyzing dewatering operations in force fields such as settling, sedimentation and filtration. However, determination of compressive yield stress by concentration profile or multiple speed equilibrium sediment height in centrifugation sedimentation technique [2,18,20] is not without its problems. Depending on centrifugal force, particle fineness and suspension chemistry, the time required for obtaining data at 5 to 6 centrifuge speeds in multiple speed equilibrium sediment height method can be in ordinarily long [15]. Moreover, the numerical inversion of data needed to extract compressive yield stress is an inherently unstable operation. This means that minor experimental errors can lead to major distortions in the results [21] unless an appropriate numerical algorithm tailored to the task is employed. Pressure filtration, on the other hand, provides a direct measurement of compressive yield stress for a given applied pressure, as evident from Eq. (5), by a reasonably straightforward experimental technique and without the intervention of any numerical–mathematical procedure. Although pressure filtration is perhaps the technique of choice for determining compressive yield stress [12,22–27] especially at intermediate and high pressures, it turns out that this method is also not without some drawbacks. The main caveat relates to time taken to reach equilibrium or near equilibrium as $\phi \rightarrow \phi_\infty$, which can be inordinately long, especially at low filtration pressures and for ultra fine colloidal suspensions and difficult to filter, biologically active materials such as municipal sludges [12].

There is a need for rapid measurement of compressive yield stress for many reasons. The yield rheology can be manipulated by altering solution chemistry of the suspension for possible improvement in its dewatering characteristics, especially the end point moisture. This invariably entails trial and error screening of reagents – and establishment of optimal dosage – by monitoring compressive yield stress at different pressures. A minimum of five to seven pressures is needed for a meaningful curve fitting of data to an empirical function for $P_y(\phi)$. Clearly, the success of this approach depends primarily on the convenience and speed with which compressive yield stress can be determined. Fast measurement techniques are also needed in case of biologically active sludges whose rheological behavior keeps changing with time and in monitoring of slurry characteristics for on-line control of industrial dewatering processes in face of fluctuating feeds. Murase et al. [25] proposed step pressure filtration as a rapid method of characterizing slurry characteristics. deKrester et al. [26] and Usher et al. [27] further developed the method and proposed two separate step pressure filtration experiments to evaluate slurry compressibility as well as its permeability. Each experiment thus comprises of a series of step pressures for rapid measurement of slope of the initial time similarity solution in Eq. (3) and compressive yield stress in Eq. (5). In latter

case, which is the focus of our work reported here, batch filtration test is conducted at lowest pressure desired until equilibrium or end point is reached as $\phi \rightarrow \phi_\infty$. Next, the pressure is stepped up to a higher level and filtration is permitted to go to equilibrium again. The pressure is incremented once more and procedure is repeated. The pressure at every step is the compressive yield stress for the solid volume fraction at equilibrium ϕ_∞. The saving in time arises from the fact that instead of carrying out single pressure filtration experiments; that is, separate filtration run for each pressure, it is sufficient to perform one filtration test at many pressures. The assumption implicit in the procedure is that the solid content of filter cake at equilibrium is path-invariant, which deKrester et al. [26] verified by comparing data from single pressure and step pressure tests and is reconfirmed in a section below.

The following points primarily motivate our work. One, as shown in the curve pertaining to the first (and lowest) applied pressure ΔP_1 in Fig. 1, a typical high pressure batch filtration run comprises, apart from a brief 'induction' period, of two stages: stage 1 for cake formation and growth which is followed by stage 2 for cake compression and consolidation. The filtration rate decreases continuously with time, becoming vanishingly small as the system approaches its end point $\phi_\infty(\Delta P_1)$. In the conventional or equilibrated step pressure method, stage 1 is skipped for all pressures except the first pressure, as seen in upper curve. Although this procedure is an improvement over the conventional single pressure method; nevertheless, only a limited reduction in the duration of the test is achieved. This is because for each pressure the process must be driven to equilibrium at steeply decreasing filtration rate. Two, the step pressure technique was proposed by deKrester et al. [26] and Usher et al. [27] for obtaining material functions needed to implement the linearized approximation to the high pressure filtration model of Landman and White [8] in Eq. (1). Interestingly, the model

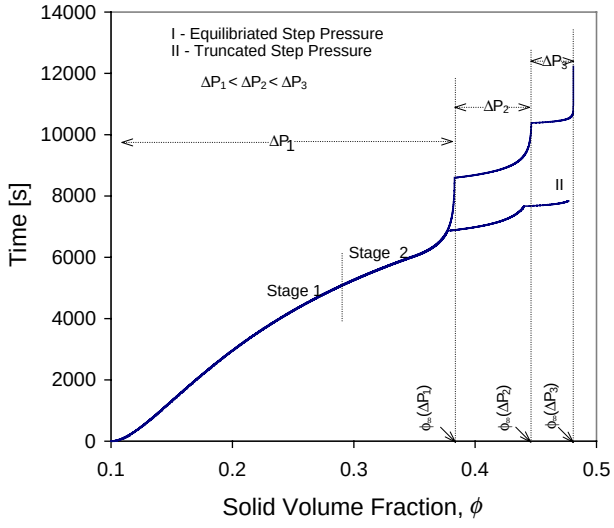

Fig. 1. Typical equilibriated and truncated step pressure filtration curves.

is not made use of in their estimation scheme. In fact, because of their fairly complex nonlinear structure, the contemporary filtration models, which explicitly incorporate multi-phase transport phenomena [5,7,11,29], are generally not suitable for identification of material functions from filtration data. The objective of our work is to address these issues. In particular, we propose rapid methods for determining compressive yield stress from truncated single pressure or truncated step pressure test data. In these experiments the filtration run is terminated in single pressure test or pressure is stepped up in multi pressure test before the system reaches equilibrium. It is evident from Fig. 1 that the truncated step pressure test shown in lower curve can be conducted in much shorter time than in the conventional equilibrated step pressure test in upper curve. In order to implement the truncated pressure technique, we utilize a simulation scheme based on $\bar{\phi}$-model, which is derived in the section that follows. We demonstrate the method by determining compressive yield stress of flocculated and dispersed suspensions. We also include the effect of polymers and surfactants on compressive yield stress over a broad range of pressures, as determined by the equilibrated step pressure method.

2. $\bar{\phi}$-model of step pressure filtration test

Details of the $\bar{\phi}$-model are given elsewhere [12,28]. Only a summary is included here for sake of providing an adequate background. Kapur et al. [12] proposed a conveniently implement-able analytical model for cake consolidation stage 2, which retains two of the most important features of the analysis of Landman and White, namely, compressive rheology of filter cake and continually shifting distribution of applied pressure over particle network stress and liquid stress. Recently, Raha et al. [28] made some modifications and improvements in the consolidation model and derived a mean-phi model. The $\bar{\phi}$-model invokes a time-invariant uniform solid volume fraction approximation for the growing filter cake in stage 1 and a time-dependent uniform solid volume fraction approximation for consolidation of filter cake in stage 2. The models for the two stages have a common physical basis, seamless continuity between the stages and mutual consistency. The model has been validated with many different kinds of high pressure filtration data. Redefining ϕ as the average solid volume fraction in the filtration chamber, the equation for stage 1 in $\bar{\phi}$-model is

$$\mathrm{d}t = \frac{2h_0^2}{\beta_\mathrm{m}^2}\frac{\phi_0}{\phi^2}\left[1-\frac{\phi_0}{\phi}\right]d\phi; \qquad \phi_0 < \phi \leq \phi_\mathrm{c} \tag{6}$$

where the rate parameter β_m^2 is given by

$$\beta_\mathrm{m}^2 = 2k\frac{(\phi_\mathrm{c}-\phi_0)(1-\phi_\mathrm{c})^3}{\phi_0\phi_\mathrm{c}^2}\Delta P \tag{7}$$

where k is a lumped permeability factor that includes pore size, tortuosity and fluid viscosity, ϕ_c is time-invariant uniform volume fraction solids in the filter cake as well as the critical solid fraction at which transition from cake formation to cake consolidation takes place at filtration time t_c and ϕ_0 is initial volume fraction solids in feed suspension. The model equation for stage 2 is

$$dt = K_m \frac{d\phi}{\phi(\phi_\infty - \phi)(1-\phi)^3}; \qquad \phi_c < \phi < \phi_\infty \tag{8}$$

with initial condition, $\phi = \phi_c$ when $t = t_c$. The lumped scalar K_m of the process time is

$$K_m = \frac{(h_0\phi_0)^2(\phi_\infty - \phi_c)}{k\Delta P} \tag{9}$$

The integrated form of Eq. (8) is

$$\begin{aligned} t = K_m \times \Bigg\{ & \frac{(\phi-\phi_c)(\phi_\infty-2)}{(\phi-1)(\phi_c-1)(\phi_\infty-1)^2} \\ & + \frac{(\phi_c-\phi)(\phi_c+\phi-2)}{2(\phi-1)^2(\phi_c-1)^2(\phi_\infty-1)} + \frac{1}{\phi_\infty}\ln\left[\frac{\phi}{\phi_c}\right] \\ & + \frac{(\phi_\infty^2 - 3\phi_\infty + 3)}{(\phi_\infty-1)^3}\ln\left[\frac{1-\phi_c}{1-\phi}\right] \\ & + \frac{1}{\phi_\infty(\phi_\infty-1)^3}\ln\left[\frac{\phi_\infty-\phi}{\phi_\infty-\phi_c}\right]\Bigg\} + t_c \end{aligned} \tag{10}$$

The implementation of $\bar{\phi}$-model requires knowledge of three process parameters: k, which is common to stage 1 and stage 2, ϕ_c, which lies at the junction of the two stages and ϕ_∞, which determines the end of the process at equilibrium.

In the step pressure filtration experiment, both cake formation (stage 1) and cake consolidation (stage 2) take place at the lowest pressure. This is followed by cake consolidation only at higher pressures. The cake formation at lowest pressure is completed at time t_c, which is given by Eq. (6) as

$$t_c = \frac{h_0^2}{\beta_{m,\,1}^2}\left(1 - \frac{\phi_0}{\phi_c}\right)^2 \tag{11}$$

where subscript 1 refers to the first level or lowest applied pressure ΔP_1. The total filtration time at lowest pressure is t_c plus the time spent in stage 2 given by Eq. (8)

$$t_{e,\,1} = t_c + K_{m,\,1}\int_{\phi_c}^{f_1\phi_{\infty,\,1}} \frac{d\phi}{\phi(\phi_{\infty,\,1} - \phi)(1-\phi)^3} \tag{12}$$

where f_1 is fraction of filter cake volume fraction solids at equilibrium $\phi_{\infty,1}$ when pressure is stepped up from first pressure to the next higher pressure. In other words, $f_1 = 1$ if the process is driven to equilibrium and $f_1 < 1$ if it is truncated before reaching steady state.

For convenience, Eq. (12) may be written as

$$t_{e,\,1} = t_c + I_1. \tag{13}$$

Similarly total filtration time at the end of second pressure stage is

$$t_{e,\,2} = t_{e,\,1} + I_2 \tag{14}$$

In general, at end of the n-th pressure stage

$$t_{e,\,n} = t_{e,\,n-1} + I_n \tag{15}$$

By successive substitutions

$$t_{e,\,n} = t_c + \sum_{j=1}^{n} I_j \tag{16}$$

where from Eqs. (8), (9), (12) and (13)

$$\begin{aligned} I_1 = & \frac{(h_0\phi_0)^2(\phi_{\infty,\,1} - \phi_c)}{k_1\Delta P_1} \\ & \times \int_{\phi_c}^{f_1\phi_{\infty,\,1}} \frac{d\phi}{\phi(\phi_{\infty,\,1} - \phi)(1-\phi)^3} \end{aligned} \tag{17}$$

and for $j = 2,3,\ldots, n$

$$\begin{aligned} I_j = & \frac{(h_0\phi_0)^2(\phi_{\infty,\,j} - \phi_{\infty,\,j-1})}{k_j\Delta P_j} \\ & \times \int_{f_{j-1}\phi_{\infty,\,j-1}}^{f_j\phi_{\infty,\,j}} \frac{d\phi}{\phi(\phi_{\infty,\,j} - \phi)(1-\phi)^3} \end{aligned} \tag{18}$$

where the integral terms in Eqs. (17) and (18) can be evaluated by appropriate replacements in Eq. (10) after substituting $t_c = 0$ and $K_m = 1$. Eqs. (16), (17) and (18) constitute the model equations for step pressure filtration test.

3. Experimental

Particulate suspensions for pressure filtration tests were prepared from A16 SG alumina of mean particle size 0.4 μm (supplied by Alcoa-ACC Industrial Chemical Ltd, India). Poly acrylic acid of various molecular weights, sodium oleate and citric acid were employed as reagents for altering the rheology and filtration characteristics of suspensions. 4 N NaOH and 4 N HNO_3 were used to adjust the pH. The suspensions were prepared by dispersing the powder with a magnetic stirrer for 2 min, followed by ultrasonication with a Branson 450 sonicator for 2 min at 40 Watt power input. Whatman filter paper No. 42 was used as the filter medium. The pH of the suspension was recorded prior to its filtration. Pressure filtration experiments were carried out in a highly instrumented, programmable computer -driven laboratory scale test rig, which has been described in details elsewhere by its designers [26].

The model parameters were estimated by fitting the integrated forms of $\bar{\phi}$-model; that is, Eqs. (6) and (8) to single pressure filtration data or Eqs. (11) and (16) to step pressure filtration data, by minimizing the sum of the

squares of errors by a nonlinear optimization routine called SUMT.

3.1. Procedure for the proposed fast estimation scheme for ϕ_∞ by step pressure method

The pressure filtration model in Eqs. (6) and (8) has three parameters namely, lumped permeability factor (k), critical average solid volume fraction, ϕ_c at transition from stage 1 to stage 2 and the end point solid volume fraction ϕ_∞ when equilibrium is reached and filtration ceases. The compressive yield stress of the dewatered slurry at ϕ_∞ is simply the applied filtration pressure.

The measurement of ϕ_∞ can be very time consuming because of extremely slow approach to the equilibrium, especially in case of fine and colloidal suspensions. The procedure for the proposed fast estimation scheme for ϕ_∞ is as follows:

- Measure ϕ_o, the initial solid volume content in the suspension feed.
- Measure effluent per unit area (V) as a function of filtration time (t). Stop the test when the rate of filtration drops below a prescribed level.
- Convert $t-V$ data into $t-\phi$ data by straightforward mass balance.

$$\phi = \frac{h_0\phi_o}{h_0 - V} \tag{19}$$

- Estimate model parameters k, ϕ_c and ϕ_∞ by fitting model Eqs. (11) and (16) to experimental data. For this purpose, a nonlinear optimization scheme (SUMT) is used for minimization of a sum of squares of errors for all data points.
- Check that the experimentally measured ϕ_e, the solid volume fraction when the test is stopped, lies between estimated ϕ_c and ϕ_∞.
- Step up the pressure to next level.

The estimated ϕ_∞ by the fast procedure described above is in good agreement with the actual ϕ_∞ measured by driving the process to equilibrium after a long filtration time.

4. Results and discussion

4.1. Truncated single pressure filtration data

The objective here is to estimate ϕ_∞ using single pressure filtration data that are truncated in cake consolidation stage (i.e. $f<1$). The estimated values are compared with the benchmark or 'actual' ϕ_∞ measured directly when filtration effectively ceases as the system tends to equilibrium (i.e. $f=1$). The other two parameters of $\bar{\phi}$-model, namely, a permeability measure k and critical solid volume fraction ϕ_c are obtained concurrently in the estimation exercise. If ϕ_e ($\phi_c<\phi_e\leq\phi_\infty$) is the solid volume fraction when data is truncated (or experiment is ended), a convenient representation of the extent of data truncation is given by an index g

$$g = \frac{\phi_\infty - \phi_e}{\phi_\infty - \phi_c}; \qquad 1 > g \geq 0. \tag{20}$$

Clearly, $g=0$ when $f=1$ and no truncation is carried out, and at maximum truncation $g=1$ when no stage 2 data is utilized and parameter estimation is not possible. Fig. 2 shows the ratio of estimated and actual parameters k, ϕ_c and ϕ_∞ as a function of truncation index g. The actual parameters were determined without data truncation; that is, $g=0$. The material was flocculated suspension of A16 SG alumina at its natural pH of 9.6 and the filtration pressure was fixed at 1 kPa. It would seem that it is possible to estimate the model parameters from truncated data with reasonable accuracy. In particular, it is possible to obtain ϕ_∞ within an error of less than 1% even when the truncation index is as high as 0.5, with considerable saving in experimental time.

Fig. 3 compares experimental data and filtration curves simulated by $\bar{\phi}$-model. The parameter sets employed in simulation were estimated from experimental data truncated at $g=0$, 0.13, 0.3 and 0.5. Similar comparison is also included for filtration of a dispersed A16 SG suspension at pH 3.3 under an applied pressure of 100 kPa with parameters that were estimated from data truncated at $g=0$, 0.21, 0.38 and 0.58. The agreement is on the whole quite good even when data were drastically truncated. As an aside, note the remarkably dense cake that can be obtained when a fully dispersed suspension of this alumina is subjected to appropriate pressure and dewatering conditions. Although not exhibited here, similar results were obtained with many other systems under different filtration conditions. We may therefore conclude that $\bar{\phi}$-model-based single pressure truncated technique can accurately and

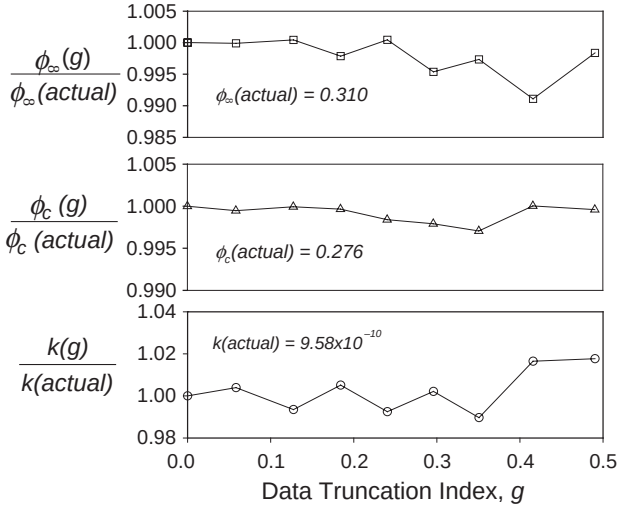

Fig. 2. Extent of errors in model parameters as a function of data truncation index g for A16 SG suspension at pH 9.6 under 1 kPa filtration pressure.

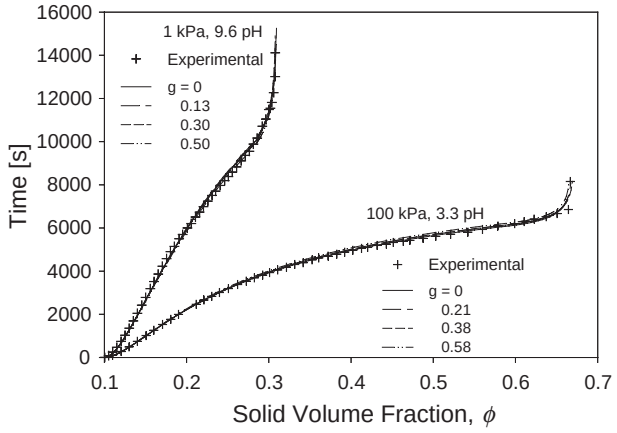

Fig. 3. Comparison of experimental and simulated A16 SG filtration curves under pH 9.6 and 1 kPa pressure and under pH 3.3 and 100 kPa pressure, using model parameters estimated from data truncated to different extent (g ranging from 0 to 0.58).

rapidly estimate the compressibility of both flocculated and dispersed suspensions over a wide range of applied pressure.

4.2. Step pressure filtration data

We first validate the step pressure filtration model in Eqs. (16), (17) and (18). The parameter sets needed for simulation were determined by fitting $\bar{\phi}$-model to single pressure filtration data for 5, 25 and 100 kPa pressures. Comparison of experimental data and simulated step pressure plots in Fig. 4 show good overall agreement in case of the conventional step pressure experiment where filtration is driven to equilibrium at each pressure level.

Fig. 5 shows a composite compressive yield stress curve of A16 SG made from single pressure test data and four sets of step pressure test data, all carried out to equilibrium. The sets differed from one another in number of steps as well as magnitude of pressures. To a first approximation, the data

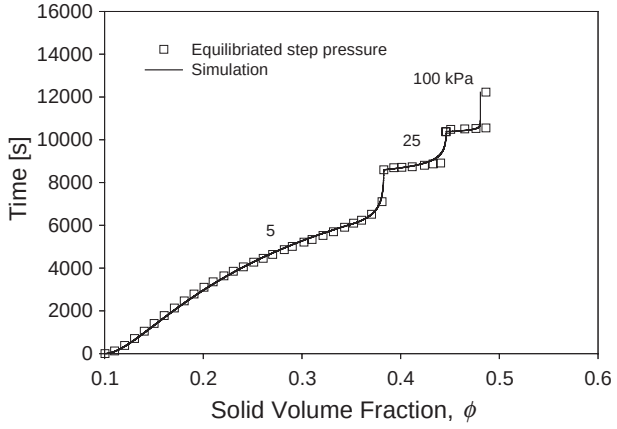

Fig. 4. Experimental data and simulated equilibriated step pressure filtration curve of A16 SG suspension. The step pressures employed were 5, 25 and 100 kPa and model parameters were estimated from single pressure filtration tests same pressures.

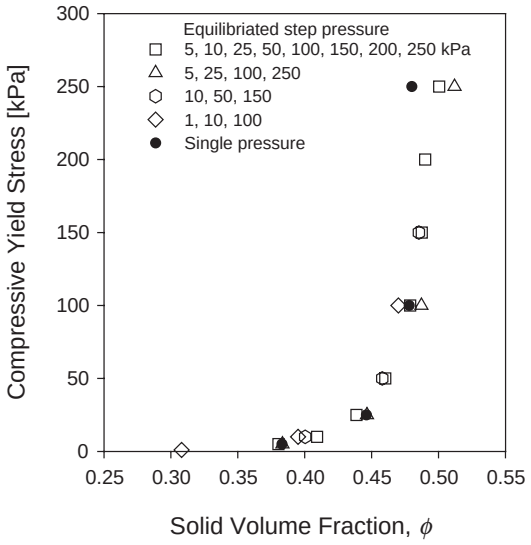

Fig. 5. Compressive yield stress curves of A16 SG obtained from four different sets of step pressures experiments and single pressure filtration runs.

points obtained under different experimental protocols collapse onto a single curve. This result suggests that compressive yield stress is a material property which is path invariant and, as shown elsewhere, independent of initial solid loading of suspension and its height in filtration chamber [12,15,18,26]. These conclusions are, however, subject to some qualifications. For example, it is known that, although independent of the pressure history, ϕ_∞ depends on the method employed for preparation of the suspension and its microstructure [17]. Moreover, there is experimental evidence to suggest that, for reasons not understood, test suspensions whose solid loadings lie below the gel point could give rise to variable and in general lower ϕ_∞ than those above the gel point [12,26].

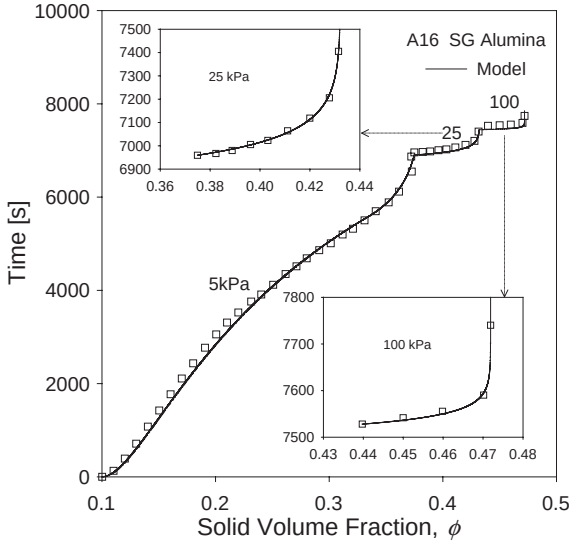

Fig. 6. Experimental data and simulated truncated step pressure filtration curve of A16 SG suspension under 5, 25 and 100 kPa pressures.

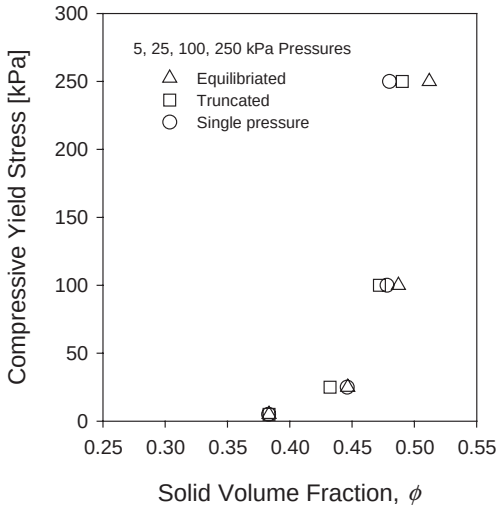

Fig. 7. Compressive yield stress curves of A16 SG obtained from single pressure, equilibrated and truncated step pressure tests.

Fig. 6 shows the fit of $\bar{\phi}$-model to experimental data for truncated step pressure filtration of A16 SG suspensions when pressure is stepped up from 5 to 25 and then 100 kPa at f=0.973, 0.967 and 0.970, respectively. The quality of simulation achieved is more evident in the two expanded views inserted in the figure. A comparison of Figs. 4 and 6 reveals that even though f>0.96 there is considerable difference in total times required to complete the equilibrium and truncated step pressure tests. These results suggest that it should be able to extract compressive yield stress as a function of applied pressure from truncated step pressure data with considerable saving in experiment time.

Fig. 7 compares the compressive yield stress of A16 SG estimated from single pressure, equilibriated step pressure and truncated step pressure tests. It may be concluded that the truncated step pressure data can be used in conjunction with $\bar{\phi}$-model for rapid estimation of compressive yield stress with reasonable accuracy.

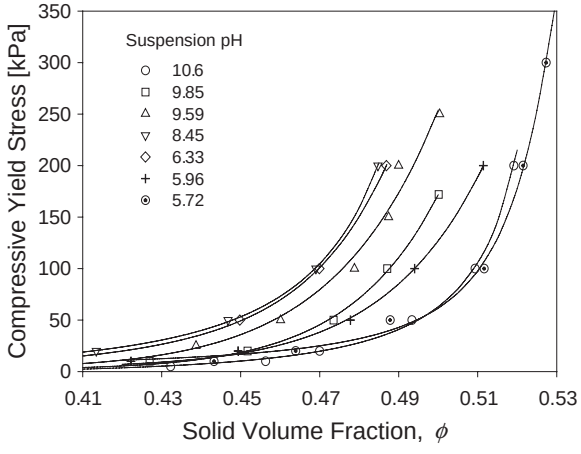

Fig. 8. Compressive yield stress curves of A16 SG obtained from step pressure filtration tests under various pH conditions.

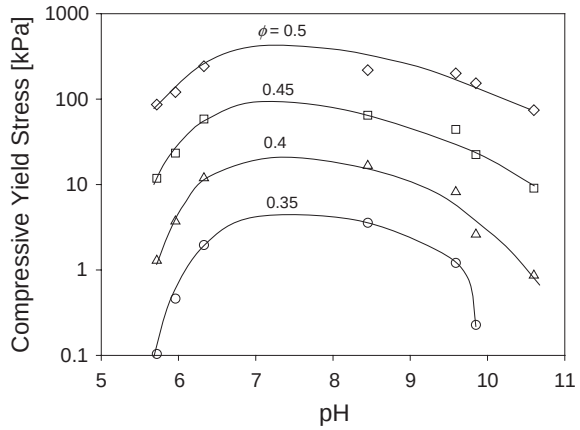

Fig. 9. Compressive yield stress of A16 SG under various pH conditions for different solid loadings.

Effect of suspension pH on compressibility has been investigated in the past by centrifugal consolidation and single pressure filtration techniques. The reported data are somewhat limited in scope, presumably because of time-consuming nature of the measurements [15,24]. We have used the step pressure filtration method for a detailed study of the pH effect on compressibility. Fig. 8 shows a family of compressive yield stress curves for A16 SG suspensions at various pH. The right hand side curves of the most dispersed suspensions of the set at pH 5.72 and 10.6 exhibit highest compressibility. The flocculated or mostly flocculated suspensions in range of 6.33 to 8.45 pH on the left hand side show the least compressibility. An alternate and perhaps clearer representation of the data is given in Fig. 9 where compressive yield stress is plotted as a function of pH for various ϕ values. As pH increases from less than 6 (acidic medium) to more than 10 (alkaline environment), compressive yield stress initially increases sharply (compressibility decreases), goes through a broad, almost flat plateau and finally drop steeply. This trend is consistent with dispersed–flocculated–dispersed state of the alumina suspension as its pH is varied from 5.72 to 10.6. The maximum

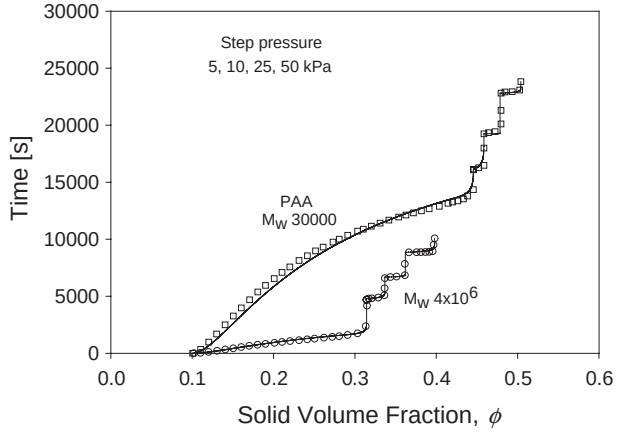

Fig. 10. Step pressure filtration of A16 SG suspension with 100 ppm PAA of low and high molecular weights.

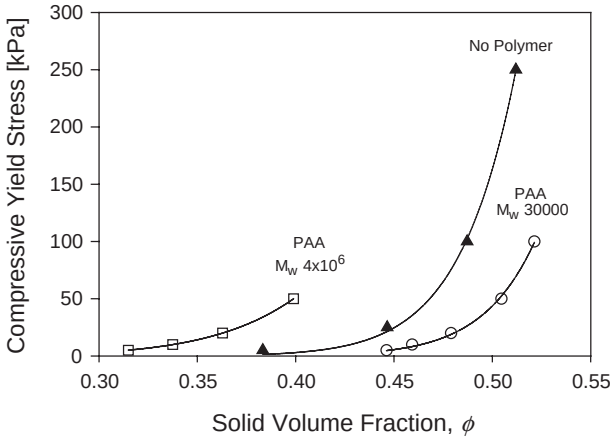

Fig. 11. Effect of 100 ppm PAA of low and high molecular weight on compressive yield stress of A16 SG.

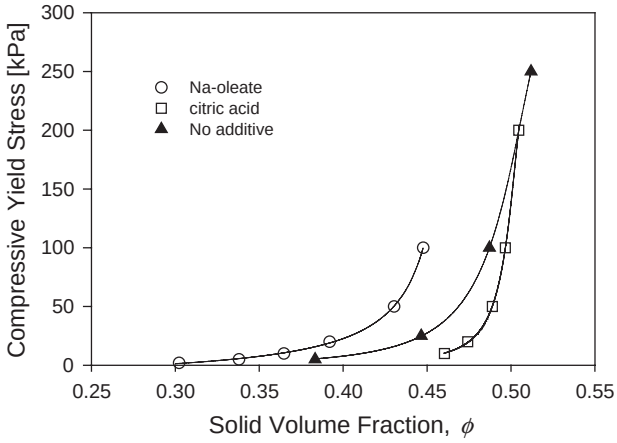

Fig. 13. Effect of 100 ppm Na-oleate and citric acid on compressive yield stress of A16 SG.

yield stress does not lie exactly at p.z.c., which is around pH 6.5 for Alumina A16 SG sample, but is displaced by about 1.0 pH units. However, because of the flat nature of the plateau the difference is not significant. Similar mismatch was also observed between p.z.c. and shear yield stress of suspensions [30].

Industrial use of polymer flocculants is common in preprocessing of fine and colloidal suspensions before dewatering. As pointed out above, rapid determination of cake compressibility and permeability in presence of polymers reagents is essential for screening a reagent. A limited amount of quantitative data on the effect of flocculant molecular weight and dosage on compressibility was previously obtained by centrifugal consolidation and single pressure filtration with prolonged characterization times [15]. We demonstrate the faster step pressure filtration technique. Fig. 10 shows the dewatering data when 100 ppm poly acrylic acid of 30 000 and 4 million molecular weights was used in step pressure filtration tests. The time scales of filtration and the extent of dewatering are significantly different in the two cases. The rate of filtration is much faster with 4 million molecular weight polymer than with

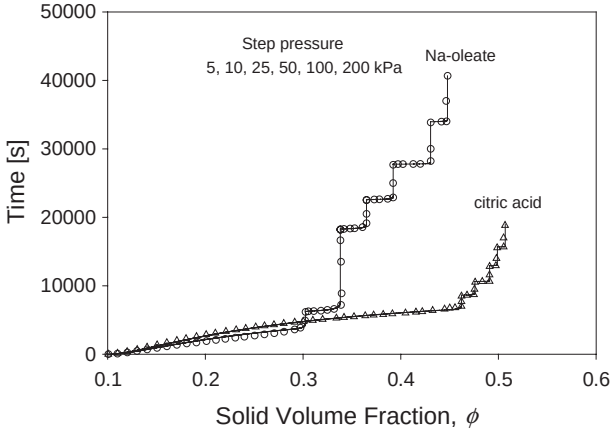

Fig. 12. Step pressure filtration curves of A16 SG suspension having 100 ppm Na-oleate and citric acid.

30 000 molecular weight polymer, but the extent of consolidation is significantly less. This is seemingly a general rule high pressure filtration, namely, dewatering kinetics is enhanced but invariably at the expense of filter cake compressibility.

The compressive yield stress curves for the two flocculants, determined from step pressure filtration tests, are shown in Fig. 11. The compressive yield stress curve without polymer addition lies between those of 30 000 and 4 million molecular weight PAA. As such, the low molecular weight polymer acts as a dispersant in this instance, slowing down the kinetics of filtration while enhancing the compressibility. On the other hand, polymer with high molecular weight acts as a bridging flocculent, resulting in faster kinetics and reduced compressibility. It turns out that apart from the choice of the polymer, the yield rheology is strongly impacted by molecular weight, dosage, even the manner of addition [31–33] and pH, all acting in concert [34,35].

Fig. 12 shows the step pressure filtration curves of A16 SG suspension with 100 ppm Na-oleate and citric acid surfactants.

Fig. 13 compares the compressive yield stress of these samples with surfactant-free suspension. As in the case of PAA polymer described in Figs. 10 and 11, compressive yield stress curve without surfactant lies between that of Na-oleate and citric acid. Citric acid acts as a dispersant, slowing down the kinetics and increasing the compressibility. Na-oleate acts as a flocculent and has the opposite effect.

5. Conclusion

In spite of its approximate nature, mean-phi model can be advantageously employed for reliable and quick estimation of compressive yield stress from truncated and or step pressure filtration tests. Based on the model, a reasonably accurate algorithm is proposed for simulation of these tests,

which makes it is possible to characterize the suspension rapidly in terms of its filtration parameters, including cake compressibility or compressive yield stress.

The technique is illustrated with step pressure filtration of colloidal suspensions in various states of aggregation and dispersion, brought on by pH adjustment and or addition of flocculants and surfactants. The extensive compressive yield stress results presented here are in broad agreement with the more limited data of previous investigators obtained by time consuming conventional characterization procedures. In general, irrespective of the manner in which the state of the suspension is manipulated, the dispersed suspensions lead to slower filtration kinetics but greater compressibility than flocculated suspensions which give rise to faster kinetics and lesser compressibility. It would seem that the goal of achieving enhanced filtration rate and greater extent of dewatering simultaneously by manipulation of suspension chemistry remains elusive as ever.

Notation

$D(\phi)$	Diffusion coefficient, m^2/s^{-1}
f	Fraction of equilibrium volume fraction, ϕ_∞
f_i	Fraction of equilibrium volume fraction, $\phi_{\infty,i}$, where pressure is stepped up
g	Data truncation index
h_t	Total thickness of cake and suspension, m
h_0	Initial suspension height, m
k	Lumped permeability factor including pore size, tortuosity and fluid viscosity
K_m	Lumped filtration resistance parameter of mean-phi model defined in Eq. (9)
$K_{m,i}$	Lumped filtration resistance parameter at i-th pressure level
$P_p(\phi)$	Compressive stress on particle network, kPa
$P_y(\phi)$	Compressive yield stress, kPa
$R(\phi)$	Hindered settling factor
t	Time, s
t_c	Critical filtration time, s
$t_{e,i}$	Total filtration time till the end of i-th step
V	Cumulative specific filtrate volume at filtration time t, m
z	Height from membrane

Greek letters

β	Slope of V vs. $\sqrt{t}$ plot, $m/s^{0.5}$
β_m	β of mean-phi model, $m/s^{0.5}$
$\beta_{m,1}$	β of mean-phi model at lowest pressure, $m/s^{0.5}$
ΔP	Applied pressure, kPa
ΔP_i	Applied pressure at i-th step of step pressure filtration, kPa
ϕ	Local or average solid volume fraction
ϕ_c	Critical average solid volume fraction
ϕ_e	Solid volume fraction at data truncation
ϕ_g	Solid volume fraction at gel point
ϕ_∞	Maximum solid content of cake at an applied pressure
$\phi_{\infty,i}$	Maximum solid content of cake at an applied pressure ΔP_i
ϕ_0	Initial solid volume fraction
$\bar{\phi}$	Uniform solid volume fraction in cake
$\kappa(\phi)$	Dynamic compressibility defined in Eq. (4)

Acknowledgement

Financial support for this work from the Department of Science and Technology (DST), Govt. of India is gratefully acknowledged. We are grateful to Prof. Mathai Joseph, Executive Director, TRDDC for encouragement and support. The authors are grateful to one of the reviewers for providing valuable inputs on the intricacies of step pressure filtration methodology.

References

[1] M. Shirato, T. Murase, M. Iwata, in: R.J. Wakeman (Ed.), Progress in Filtration and Separation, 4th ed., Elsevier, Amsterdam, 1986, p. 181.
[2] R. Buscall, L.R. White, J. Chem. Soc., Faraday Trans. 1 83 (1987) 873.
[3] R.J. Wakeman, M.N. Sabri, E.S. Tarleton, Powder Technol. 65 (1991) 283.
[4] K.A. Landman, C. Sirakoff, L.R. White, Phys. Fluids, A Fluid Dyn. 3 (1991) 1495.
[5] K.A. Landman, L.R. White, M. Eberl, AIChE J. 41 (1995) 1687.
[6] K.A. Landman, J.M. Stankovich, L.R. White, AIChE J. 45 (1999) 1875.
[7] R.G. Holdich, IJMP 39 (1993) 157.
[8] K.A. Landman, L.R. White, AIChE J. 43 (1997) 3147.
[9] F.M. Tiller, J.H. Kwon, AIChE J. 44 (1998) 2159.
[10] H. Sis, S. Chander, Miner. Metall. Process. 17 (2000) 41.
[11] R. Burger, F. Concha, K.H. Karlsen, Chem. Eng. Sci. 56 (2001) 4537.
[12] P.C. Kapur, S. Raha, S. Usher, R.G. de Krester, P.J. Scales, J. Colloid Interface Sci. 256 (2002) 216.
[13] R. Buscall, P.D.A. Mills, J.W. Goodwin, D.W. Lawson, J. Chem. Soc., Faraday Trans 1 84 (1988) 4249.
[14] G.H. Meeten, Colloids Surf., A Physicochem. Eng. Asp. 82 (1994) 77.
[15] M.D. Green, D.V. Boger, Ind. Eng. Chem. Res. 36 (1997) 4984.
[16] G.M. Channell, C.F. Zukoski, AIChE J. 43 (1997) 1700.
[17] G.M. Channell, K.T. Miller, C.F. Zukoski, AIChE J. 46 (2000) 72.
[18] K.T. Miller, R.M. Melant, C.F. Zukoski, J. Am. Ceram. Soc 79 (1996) 2545.
[19] L.A. Brown, C.F. Zukoski, AIChE J. 49 (2003) 362.
[20] M.D. Green, M. Eberl, K.A. Landman, AIChE J. 42 (1996) 2308.
[21] Y.L. Yeow, Y.K. Leong, AIChE J. 47 (2001) 2798.
[22] M. Eberl, K.A. Landman, P.J. Scales, Colloids Surf., A Physicochem. Eng. Asp. 103 (1995) 1.
[23] M.D. Green, K.A. Landman, R.G. de Krester, D.V. Boger, Ind. Eng. Chem. Res. 37 (1998) 4152.
[24] A.A.A. Aziz, R.G. de Krester, D.R. Dixon, P.J. Scales, Water Sci. Technol. 14 (2000) 9.
[25] T. Murase, E. Iritani, J.H. Cho, M. Shirato, J. Chem. Eng. Jpn. 22 (1989) 373.
[26] R.G. de Krester, S.P. Usher, P.J. Scales, D.V. Boger, AIChE J. 47 (2001) 1758.
[27] S.P. Usher, R.G. de Krester, P.J. Scales, AIChE J. 47 (2001) 1561.
[28] S. Raha, K.C. Khilar, Pradip, P.C. Kapur, Can. J. Chem. Eng. (submitted for publication).

[29] N.M. Abboud, M.Y. Corapcioglu, J. Colloid Interface Sci. 160 (1993) 304.
[30] P.J. Scales, S.B. Johnson, T.W. Healy, P.C. Kapur, AIChE J. 44 (1998) 538.
[31] R.O. Keys, R. Hogg, AIChE Symp. Ser. 75 (1979) 190.
[32] R.C. Klimpel, R. Hogg, J. Colloid Interface Sci. 113 (1986) 121.
[33] R. Hogg, R.C. Klimpel, D.T. Ray, Miner. Metall. Process. 4 (1987) 108.
[34] P.J. Scales, S.B. Johnson, P.C. Kapur, Miner. Process. Extr. Metall. Rev. 20 (1999) 27.
[35] M. Subbanna, P.C. Kapur, Pradip, Ceram. Int. 28 (2002) 401.